Interferometric diameter determination of a silicon sphere using a traceable single laser frequency synthesizer

2013 Meas. Sci. Technol. 24 115202

(http://iopscience.iop.org/0957-0233/24/11/115202)

Meas. Sci. Technol. **24** (2013) 115202 (8pp) doi:10.1088/0957-0233/24/11/115202

Interferometric diameter determination of a silicon sphere using a traceable single laser frequency synthesizer

Xuejian Wu, Yan Li, Haoyun Wei, Honglei Yang, Guoce Yang and Jitao Zhang

State Key Lab of Precision Measurement Technology and Instruments, Department of Precision Instrument, Tsinghua University, Beijing 100084, People's Republic of China

E-mail: wu-xj09@mails.tsinghua.edu.cn

Received 28 June 2013, in final form 12 August 2013
Published 25 September 2013
Online at stacks.iop.org/MST/24/115202

Abstract
To determine the absolute diameter of a silicon sphere for the Avogadro constant project, we present a phase-shifting interferometer based on a flat etalon and a traceable single laser frequency synthesizer. By using an optical frequency comb to calibrate a frequency-tunable diode laser, the single laser frequency synthesizer can produce an arbitrary laser frequency with a relative uncertainty of 9.2×10^{-12} in the range of 4 THz. According to the laser frequency tuning system, the Carré algorithm with arbitrary but equal phase steps is employed to calculate the fractional interference phases. The absolute diameter is obtained by measuring the fractional and integral parts based on the principles of phase-shifting interferometry and frequency-sweeping interferometry, respectively. The uncertainty of a single diameter measurement in air is estimated to be 5 nm, whose uncertainty sources from the laser frequency and the phase-shifting algorithm are negligible.

Keywords: Avogadro constant, diameter, interferometry, frequency-tunable diode laser, optical frequency comb

(Some figures may appear in colour only in the online journal)

1. Introduction

The Avogadro constant N_A is the number of constituent particles in a mole of a pure substance, which is closely related to the Planck constant and some of the SI base units, such as the kilogram and mole [1]. For a possible method of redefinition of the kilogram, the collaborative research of N_A determination has been conducted by the International Avogadro Coordination (IAC) consisting of several national metrology institutes with a target relative uncertainty of 2×10^{-8} for the past decade. To date, the most accurate N_A is determined by the use of the x-ray crystal density (XRCD) method to count the atoms in a 1 kg single crystal sphere with a relative uncertainty of 3×10^{-8} [2]. According to the XRCD method, N_A can be calculated from the lattice parameter, mean molar mass, volume and mass of a single crystal silicon sphere, whose measurement principle is to determine the ratio of the atomic and the macroscopic densities of the substance. Currently, the accuracy of N_A is limited by the uncertainty of the sphere volume, whose relative uncertainty is 2.9×10^{-8} [2]. For volume determination, the absolute diameter of the silicon sphere is actually measured by laser interferometry. Thanks to the polishing technique of silicon sphere manufacturing, asphericity can be easily restricted within 100 nm so that the volume error caused by asphericity is less than 10^{-11} by calculating the volume using the mean diameter from many directions [3, 4]. To meet the requirement of the kilogram redefinition, the uncertainty of interferometric diameter determination should be reduced to 0.3 nm corresponding to a relative uncertainty of 1×10^{-8} for the sphere volume, but the current uncertainty is ~1 nm for the 93.6 mm diameter measurement reported by IAC in 2011 [5]. Furthermore, the reliability of the diameter measurement

should be guaranteed by means of establishing at least three independent experiments [6].

The first interferometer for determining the absolute diameter of spheres was designed by Saunders to represent standards for density in 1972 [7]. The diameter of a sphere D was expressed as $D = L - (d_1 + d_2)$, where L is the length of a Fabry–Perot etalon, d_1 and d_2 are the separations of the sphere from each of the etalon faces, respectively, measured by analyzing the static interferograms. Since the 1990s, different types of interferometers [8–15] have been developed to measure the absolute diameter of the silicon sphere based on Saunders' principle. According to the configuration of Fabry–Perot etalons, interferometers can be divided into two categories, the spherical etalon interferometer [14] and the flat etalon interferometer [15]. The spherical Fizeau interferometer can measure about 10 000 diameters of the sphere in an aperture angle of 60° simultaneously, because a spherical etalon is placed in two Fizeau lenses to generate a spherical wave. However, wavefront distortions caused by the spherical etalon contribute ~95% to the total uncertainty [14]. In contrast, the flat etalon interferometer avoids the wavefront aberration and enhances the alignment accuracy [15], which is an easier and more accurate scheme for a single diameter measurement. In terms of measuring methods, phase-shifting interferometry [16] is used in all the interferometers to obtain sub-nanometer accuracy of the absolute distances. In previous interferometers [8–10], phase shifts were generated by means of a mechanical scanning method based on a piezoelectric transition or a monolithic flexure hinge mechanism. Nowadays, a frequency-tunable diode laser calibrated by an iodine-stabilized He–Ne laser is used to produce more accurate phase shifts using laser frequency sweeping in a range of several GHz [11–15]. However, to achieve the diameter uncertainty of 0.3 nm corresponding to $\lambda/2000$, novel flat etalon interferometers need to be invented to reduce the uncertainties from interferogram analysis [15] and laser beam diffraction effect [17, 18].

In this paper, we present a phase-shifting interferometer to determine the absolute diameter of a silicon sphere based on a flat etalon and a traceable single laser frequency synthesizer. The absolute diameter is attained by combining the fractional and integral measurement results, which are measured by the principles of phase-shifting interferometry and frequency-sweeping interferometry using laser frequency tuning, respectively. An optical frequency comb (OFC) is exploited as a laser frequency ruler to measure and control the frequency of an external cavity diode laser (ECDL), so that the uncertainties of the laser frequency and the phase step are insignificant. The Carré algorithm with arbitrary but equal phase steps is used to calculate the fractional interference phases according to the characteristic of the single laser frequency synthesizer. The diameter measurement process, results and uncertainty budget are detailed in this paper.

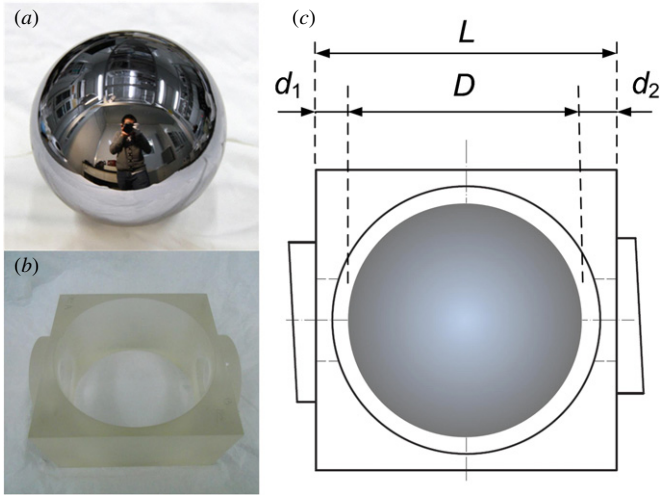

Figure 1. (*a*) Photo of the silicon sphere. (*b*) Photo of the etalon. (*c*) Schematic of the diameter measurement.

2. Experimental setup

2.1. Silicon sphere and Fabry–Perot etalon

A 1 kg single crystal silicon sphere fabricated at the China Precision Engineering Institute for Aircraft Industry is used in our experiment, as shown in figure 1(*a*). The nominal diameter is 93.626 (5) mm measured by a three-coordinate measuring machine from HEXAGON Metrology and the asphericity is measured to be 84 nm. The Ra value of the silicon sphere roughness is 1.0 nm, measured by a white-light interferometer from Zygo. These parameters ensure that the diameter measurement uncertainty from the silicon sphere is negligible. As shown in figure 1(*b*), the Fabry–Perot etalon, made of ultra-low expansion glass (Corning, 7972) with a linear thermal expansion coefficient of $3 \times 10^{-8}\,\mathrm{K}^{-1}$, consists of a cuboid spacer and two circular flat plates and serves as a length standard. The cuboid spacer (108 mm wide and 60 mm high) has a vertical hole (98 mm diameter) to place the silicon sphere and a horizontal hole (20 mm diameter) to introduce the laser beams. Either circular flat plate (30 mm diameter and 10 mm thickness), serving as a reference surface, has a 12 mrad wedge between the two surfaces to eliminate spurious light reflection from the outer surface. Besides, the flat plates are uncoated to match the low reflectivity of the silicon sphere and decrease multiple-beam interference. The circular flat plates are fixed at the end faces of the cuboid spacer by optical wringing so that the inner surfaces of the plates are parallel to each other within 5 μrad, ensured by the polishing process of the cuboid spacer. Thus, as shown in figure 1(*c*), the diameter of the silicon sphere is expressed as $D = L - (d_1 + d_2)$, where L is the distance between the two inner surfaces of the flat plates, and d_1 and d_2 are the gaps between the sphere and the respective inner surface of the flat plates. In our experimental setup, the nominal distances of L and $(d_1 + d_2)$ are 108.013 (5) mm and 14.387 (5) mm, respectively. Since the reflected wave from the plate is plane and the reflected wave from the sphere is spherical, the short gap distances make sure that appropriate visibility of the interference fringes can be observed after a focusing lens.

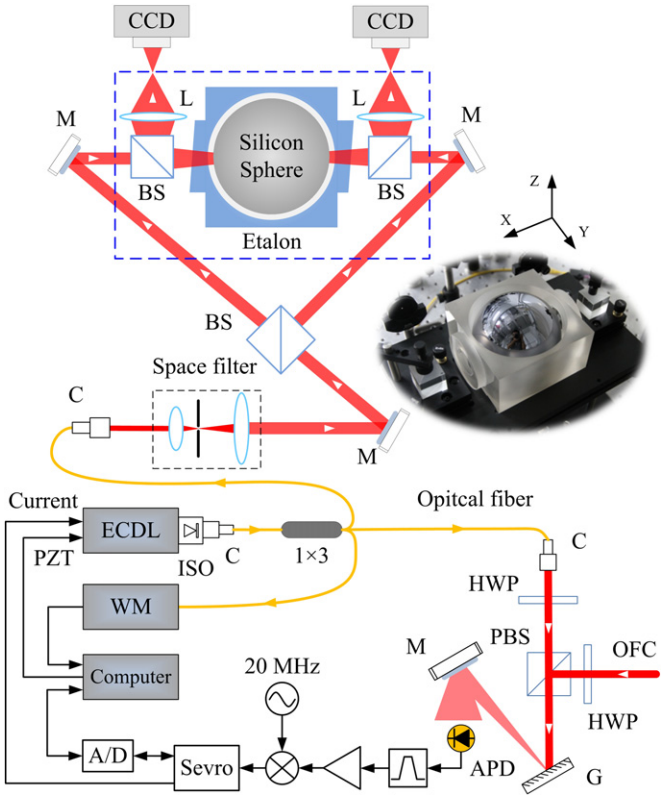

Figure 2. Experimental setup of the phase-shifting interferometer for silicon sphere diameter determination. L: lens; BS: beamsplitter; M: mirror; ISO: isolator; C: collimator; HWP: half wavelength plate; PBS: polarized beamsplitter; APD: avalanche photodetector; G: grating; WM, wavelength meter.

2.2. Interferometer

The schematic of the phase-shifting interferometer, illustrated in figure 2, consists of a flat etalon interferometer and a single laser frequency synthesizer. The laser from the ECDL (New Focus, TLB6304) is divided into three ports using an optical fiber coupler, the first part used for illuminating the flat etalon interferometer, the second part used for beating with the OFC and the third part used for monitoring the wavelength. For the flat etalon interferometer, the working laser from a fiber collimator passes through a spatial filter with a beam diameter of 4.2 mm and is then divided into two beams to illuminate the etalon and the sphere oppositely. The etalon and the sphere are mounted in a chamber with passive thermal control to ensure a stable measurement environment in air. The reflected beams are focused by a lens with focal length 45 mm. The distance between the plate and the lens is ∼190 mm, and the distance between the CCD camera and the lens is ∼310 mm. To measure the gap distances, d_1 and d_2, the silicon sphere is placed on a three-pin stage and adjusted to the center of the etalon. The interferograms generated by the reflection from either inner surface of the plates and the surface of the silicon sphere are acquired by the two 12-bit digital CCD cameras (UNIQ, UP1830), respectively. On the other hand, to measure the length of the etalon, L, one of the two beams is shut off and the silicon sphere is lifted out of the etalon by a stage. The interferograms generated by the reflection from the inner surfaces of the plates are acquired by one CCD camera.

In the etalon length measurement, misalignment between the laser beams and the etalon can result in cosine errors. Thus, the incident angles and positions of the two opposite propagation beams should be precisely adjusted by the mirrors to ensure that the direction of the laser beams is perpendicular to the inner surfaces of the plates and the two incident laser beams propagate in the same path along the etalon. As the sphere is lifted out of the etalon and the two beams illuminate the etalon oppositely, the interferogram produced by the reflection of the two inner surfaces of the plates and one opposite propagation beam is acquired by the CCD camera. First, by the use of the geometrical optics principle, adjust the position and the angle of the mirrors to make the incident beams and the reflected beams overlap both at the center of the plates and on the plane of the CCD camera. Thus, the alignment has been adjusted coarsely. Afterward, by use of the physical optics principle, adjust the angle of the mirrors slightly to optimize the alignment while observing the interferograms acquired by the CCD camera. It is an indication that the optimal alignment has been obtained when only the sparsest interference fringes are observed. By shutting off one of the incident beams, the angle of the reflection from the two inner surfaces of the plates and the common path of the two incident beams can be optimized, respectively. However, there is still an alignment uncertainty caused by the non-absolute perpendicular between the incident beams and the plates. To evaluate the alignment uncertainty, the angle between the incident beams and the plates is measured by means of the Zernike polynomials fitting the interference phase map of the reflection from the inner surfaces of the plates. The phase map is calculated by phase-shifting interferometry, which is detailed in section 3.1. The angle between the incident beams and the plates is measured to be within 10 μrad for any alignment process. Therefore, considering the angle of the two plates, the error of the alignment for the flat etalon interferometer is found to be 11 μrad.

A single laser frequency synthesizer consisting of a beat signal detection unit and feedback loop circuits is used for laser frequency stabilization and phase shift generation. A commercial OFC (Menlo System, FC1500-250) based on an erbium-doped mode-locked fiber laser is employed as a laser frequency ruler to lock the frequency of the ECDL. The comb spectrum at 633 nm is produced by the wavelength-shift process and the second harmonic generation, whose repetition rate (f_r) and offset rate (f_o) are locked to an Rb clock (Symmetricom, 8040C) at 250 MHz and 20 MHz, respectively. The beat rate (f_b), the frequency difference between the ECDL and the adjacent comb mode, is detected and locked to the Rb clock at 20 MHz. Thus, the absolute frequency of the locked ECDL can be expressed as $f = Nf_r - 2f_o + f_b$, where N is the integer of the comb mode measured by the wavelength meter (Highfinesse, WS-7) with an accuracy of 60 MHz; the signs are determined by changing the repetition rate and observing the variation of the beat rate. To generate arbitrary single laser frequency, the frequency of the ECDL can be locked to different comb modes with a frequency step

of 250 MHz. On the other hand, to produce laser frequency tuning with smaller steps, the frequency of the ECDL can be locked to a specific comb mode and the repetition rate of the frequency comb can be scanned. Then, the frequency of the ECDL can be tuned continuously as the comb mode scans. The spectrum of the frequency comb at 633 nm is larger than 10 nm, so the frequency tuning range of the single laser frequency synthesizer is over 3 THz, which is determined by the wavelength tuning range of the ECDL. Details of the ECDL locking system can be found in [19].

To investigate the uncertainty of the single laser frequency synthesizer, the ECDL is locked to the 1894 449th comb mode. The mean absolute frequency is 473 612 230 MHz. The single laser frequency synthesizer is referenced to the Rb clock, whose frequency uncertainty is 0.4 mHz. For an averaging time of 0.03 s corresponding to the shutter time of the CCD camera, the standard deviations of the repetition rate, the offset rate and the beat rate are 2.3 mHz, 0.5 Hz and 0.4 Hz, respectively, as shown in figure 3. Therefore, the frequency uncertainty of the locked ECDL is 4.4 kHz, which corresponds to a relative uncertainty of 9.2×10^{-12}.

3. Interferometric measurement

3.1. Fractional diameter measurement

To calculate the fractional interference phase from the interferograms, a phase-shifting algorithm that is appropriate for the method of the phase-shift generation is necessary. Various phase-shifting algorithms have been reviewed in [16]. Generally, phase-shifting algorithms consist of two categories, synchronous algorithms with known phase steps and asynchronous algorithms with arbitrary but equal phase steps. All national metrology institutes employ synchronous phase-shifting algorithms in their interferometers. The symmetrical seven-step algorithm with a phase step of $\pi/3$ is used by the National Metrology Institute of Japan (NMIJ, Japan) [12] and the National Measurement Institute (NMIA, Australia) [13]. A modified five-step algorithm with low sensitivity to phase step errors is used by the National Institute of Metrology (NIM, China) [10]. The cross four-step algorithm with a phase step of $\pi/2$ is employed by the Physikalish-Technische Bundesanstalt (PTB, Germany) [12]. However, the phase step error in synchronous algorithms is inescapable, because phase steps are produced by laser frequency tuning and the laser frequency variation corresponding to an interference cycle cannot be known exactly. In contrast, asynchronous phase-shifting algorithms with arbitrary but equal phase steps are more welcome in our phase-shifting interferometer. The Carré algorithm is the most often used algorithm with an arbitrary phase step [20]. Recently, multi-step phase-shifting algorithms with an unknown but constant phase step were derived from the Carré algorithm to suppress phase measurement errors from the phase shift miscalibration [21, 22].

The fractional interference phase retrieved by the Carré algorithm is expressed as

$$\tan\varphi(x, y) = \left[\frac{(3I_2 - 3I_3 - I_1 + I_4)(I_1 + I_2 - I_3 - I_4)}{(I_1 - I_2 - I_3 + I_4)^2}\right]^{1/2}, \quad (1)$$

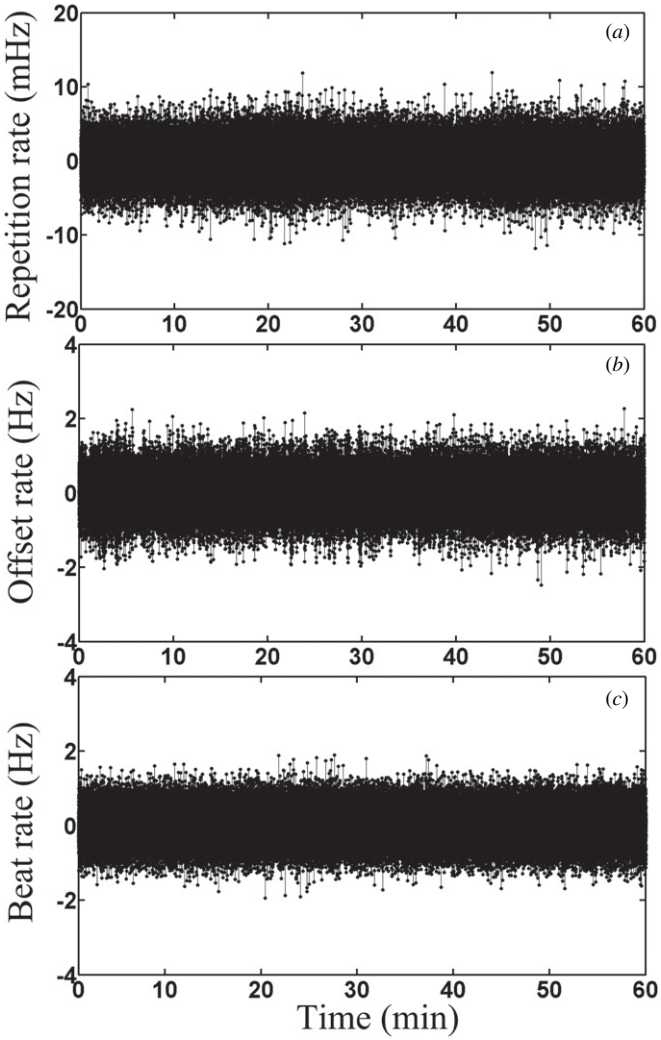

Figure 3. For an integration time of 0.03 s, (*a*) is the repetition rate variation with the mean frequency of 250 MHz and the standard deviation of 2.3 mHz; (*b*) is the offset rate variation with the mean frequency of 20 MHz and the standard deviation of 0.5 Hz; (*c*) is the beat frequency variation with the mean frequency of 20 MHz and the standard deviation of 0.4 Hz.

where I_1, I_2, I_3 and I_4 are the interferograms acquired by the CCD camera as the laser frequency is tuning with an interval corresponding to an interference phase step of 2α. The phase step 2α can be arbitrary except for $m\pi$, where m is an integer. The phase calculated from (1) is wrapped in the range of $[0, \pi/2]$, but the fractional phase required for calculating the fractional diameter should be in the range of $[0, 2\pi]$. To unwrap the phase distribution into one interference cycle of $[0, 2\pi]$, the phase step should be known roughly to determine the quadrants of the phase using the equations

$$I_2 - I_3 = (2b\,\sin\alpha)\sin\varphi, \quad (2)$$

$$I_2 + I_3 - I_1 - I_4 = (8b\cos\alpha\sin^2\alpha)\cos\varphi. \quad (3)$$

Then, the phase distribution can be unwrapped into one interference cycle of $[0, 2\pi]$ by adding 0, $\pi/2$, π or $3\pi/2$ according to the quadrants of each pixel.

In our phase-shifting interferometer based on laser frequency tuning, the phase step 2α can be expressed as

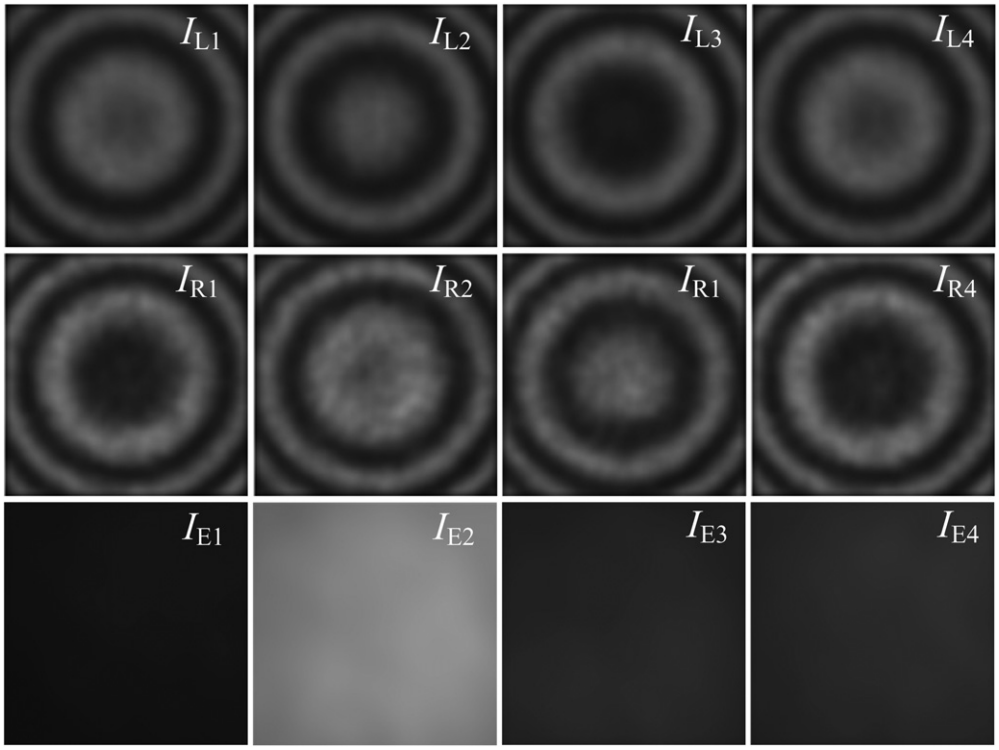

Figure 4. Phase-shifting interferograms. I_{L1}, I_{L2}, I_{L3} and I_{L4} are the interferograms produced by the reflection from the left plate and the silicon, I_{R1}, I_{R2}, I_{R3} and I_{R4} are the interferograms produced by the reflection from the right plate and the silicon, and I_{E1}, I_{E2}, I_{E3} and I_{E4} are the interferograms produced by the reflection from the plates of the etalon. For the interferograms of the gaps, the laser frequency interval is 6.5 GHz. For the interferograms of the etalon, the laser frequency interval is 500 MHz. The central laser frequency is 473.612 230 THz.

$$2\alpha = 2\pi \frac{2nl}{c} \Delta\nu, \tag{4}$$

where l is the nominal distance to be measured, n is the air refractive index, c is the velocity of light and $\Delta\nu$ is the laser frequency step. Because the optical path difference is sufficiently stable, equal phase steps can be generated by equal laser frequency steps. It is recommended that a phase step of $\sim 110^\circ$ can minimize the influence of random phase noise in the Carré algorithm [20]. Thus, the laser frequency steps used for measuring the distances of the gaps and the length of the etalon are 6.5 GHz and 500 MHz, respectively, with a central laser frequency of 473.612 230 THz. The measuring process includes interferogram acquisition, phase calculation and unwrapping, diameter calculation and evaluation.

To measure the gap distances, the silicon sphere should be placed in the center of the etalon, as shown in figure 2. The silicon sphere supported by three pins can be moved along the X, Y and Z axes with a range of 4 mm by a three-axis flexure platform. On one hand, the symmetry of the concentric circular interferograms is affected by the sphere position along the Y and Z axes. On the other hand, the phase steps are affected by the sphere position along the X axis according to (4). First, the sphere position along the Y and Z axes can be optimized by observing the interferograms. To set the sphere in the center along the X axis, scan the laser frequency in a range of $\sim$21 GHz, which produces a cycle variation of the interference fringe. It indicates that the sphere is positioned in the center when the variation range of both interference fringes acquired by the two CCD cameras is one interference cycle. In other words, the gap distances d_1 and d_2 should be approximately equal. Note that an approximate central position is enough for phase-shifting interferometry because the phase steps of both gap distance measurements do not have to be exactly the same according to the Carré algorithm.

Figure 4 shows the acquired phase-shifting interferograms used for calculating the distances of the gaps and the length of the etalon. The interferograms generated by the reflection from the plates is acquired by lifting the silicon sphere up and shutting off one of the illumination beams. The spatial resolution of the interferograms is 1024 $\times$ 1024 pixels. The pixel length is 6.45 μm and the magnification factors of the gap fringes and etalon fringes are 29 and 6, respectively.

The phase distribution is calculated according to (1) and unwrapped to $[0, 2\pi]$ according to (2) and (3). By using the relation between the laser wavelength and phase, the fractional topography can be derived from the phase distribution. The laser wavelength in vacuum of 632.991 378 nm is used, and final measurement results of the diameter are corrected according to the air refractive index and the thermal expansion. Figure 5 shows the fractional topographies of the right gap, left gap and the length of the etalon, respectively. However, only a small region in the topographies is related to the sphere diameter. For the gap topography, a circular region with a center point of the maximum value and a diameter of 5 pixels is selected, whose average value stands for the fractional gap distance. Considering the pixel length and the magnification factor, the diameter measurement error caused by the averaging region is 0.003 nm. On the other hand, for

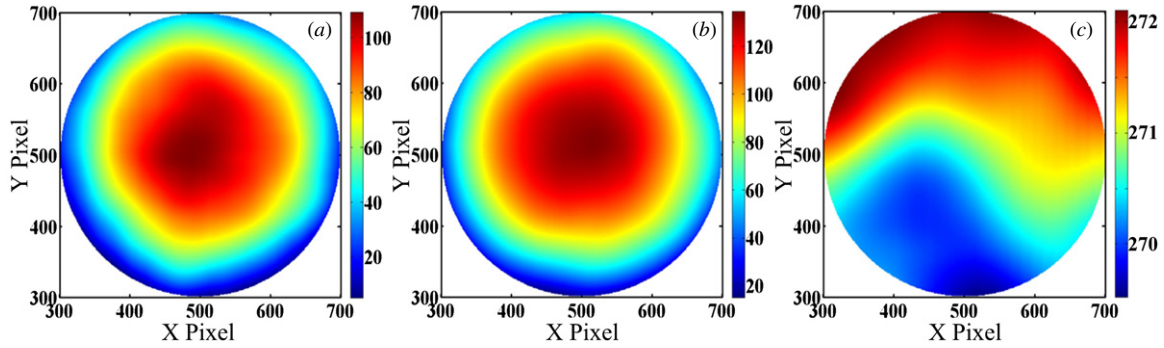

Figure 5. The fractional topographies of the right gap (*a*), left gap (*b*) and the length of the etalon (*c*). The region of the topographies is a circle with a diameter of 400 pixels in the center of the interferograms. The scale unit of the color bar is nanometer.

Table 1. Measurement result of the fractional diameter.

	Measured diameter (nm)			
Diameter	$(d_1 + d_2)$	L	D	Corrected diameter (nm)[a]
1#	210.2	260.9	50.7	183.7
2#	217.8	260.2	42.4	175.4
3#	245.1	260.8	15.7	148.7
4#	207.6	260.4	52.8	185.8
5#	226.2	260.5	34.3	167.3

[a] The fractional diameter at 20 °C and 101 kPa.

Table 2. Measurement result of the integral diameter.

Measured distances	ΔN	$\Delta\varepsilon$
L	2659	0.612
d_1	177	0.437
d_2	176	0.801

the etalon topography, the tilt angle between the two plates can be determined by the second and the third terms of the Zernike polynomials and the lateral calibration. As shown in figure 5(*c*), the tilt angle between the two plates is ∼6 μrad and the orientation is almost along the *Y* axis. The average of the same region of pixels calculated as the gap distance stands for the length of the etalon. The standard deviation of the values in the selected region is 0.01 nm.

In phase-shifting interferometry, common error sources include systematic nonsinusoidal errors of interferograms, systematic phase step errors, systematic and random intensity errors [23, 24]. Since multiple-beam interference in this interferometer is insignificant and the Carré algorithm is insensitive to all even harmonics, systematic nonsinusoidal errors are negligible. The systematic phase step error caused by the laser frequency stability of the single laser frequency synthesizer is 2.6 μrad. The laser intensity variation is less than 0.2% for the four phase steps. For a linear approximation, the phase error calculated by the Carré algorithm is proportional to the phase step error and insensitive to the background intensity variation [20]. Therefore, the phase error from the Carré algorithm is estimated to be 2.6 μrad, which corresponds to 0.0001 nm in fractional distance measurement.

Since the silicon sphere is measured in air, the air refractive index is calculated by the use of Edlen's equation with the real-time temperature (Fluke, 1523), atmospheric pressure (Setra, 470), humidity (Rotronic, HP23) and CO_2 composition (GE, TEL7001) [25]. All the sensors were carefully calibrated by NIM, and the relative uncertainty of the calculated air refractive index was found to be 2×10^{-8} [26]. Five random diameters of the silicon sphere are measured and each diameter is measured 10 times repeatedly at 23.40 °C and 100.5 kPa. Besides, the length of the etalon is also measured 10 times after each diameter measurement. As it takes only ∼10 s to acquire a series of four phase-shifting interferograms, the temperature, atmospheric pressure, humidity and CO_2 composition fluctuations are no more than 10 mK, 20 Pa, 2% and 1 ppm, respectively, during each diameter measurement process. Furthermore, the fractional diameter is corrected to 20 °C and 101 kPa using a linear thermal expansion coefficient of 2.55×10^{-6} K^{-1} [27] and a compressibility of 1.02×10^{-11} Pa^{-1} [28]. The measurement result of the fractional diameter is summarized in table 1. The standard deviation of the 10 gap measurements is ∼1 nm, which is mainly caused by the linear thermal expansion of the silicon sphere due to the short-term temperature fluctuation. Contrarily, the standard deviation of the 10 etalon measurements is ∼0.9 nm, which is mainly caused by the short-term air refractive index fluctuation. Therefore, the fractional phase measurement accuracy is better than $\lambda/600$ in the current measurement environment.

3.2. Integral diameter measurement

Before the fractional diameter measurement, the volume of the sphere is determined by means of hydrostatic weighing to obtain the integral part of the diameter in the national metrology institutes, because an ambiguity range of half a wavelength exists in phase-shifting interferometry [5]. However, the integer order ambiguity is solved by generating a temporal synthetic wavelength in our interferometer. Thus, the absolute diameter can be directly measured by laser interferometry, which simplifies the diameter measurement process. When the frequency of the ECDL is tuned continuously, the absolute distance l can be expressed as $l = c(\Delta N + \Delta\varepsilon)/2\Delta\nu$, where c is the vacuum velocity of light, $\Delta\nu$ is the frequency-sweeping range, and ΔN and $\Delta\varepsilon$ are the integral and fractional interference phase variations, respectively, according to the frequency-sweeping range [29]. Thus, the absolute distance can be obtained by measuring

Table 3. Uncertainty budget for a single diameter measurement.

Uncertainty sources	Standard uncertainty	Standard uncertainty in the diameter (nm)
Laser frequency	4.4 kHz	0.0
Phase-shifting algorithm	2.6 μrad	0.0
Fractional phase measurement	0.01 rad	1.7
Beam alignment	11 μrad	0.0
Diameter region	0.01 nm	0.0
Diffraction effect	0.02 rad	1.2
Thickness of oxide layer	0.13 nm	0.5
Surface roughness	1.0 nm	1.0
Air refractive index	2×10^{-8}	2.2
Temperature fluctuation	10 mK	2.4
Thermal expansion coefficient of silicon sphere	1×10^{-8} K^{-1}	3.2
Compressibility coefficient of silicon sphere	1.5×10^{-13} Pa^{-1}	0.0
Combined standard uncertainty		5

the frequency-sweeping range and the interference phase variations. The accuracy is relative to the frequency-sweeping range and the accuracy of the interference phase measurement.

In our interferometer, the laser frequency is tuned continuously from 470.614 230 to 474.304 230 THz, calibrated by the OFC, which corresponds to a frequency-sweeping range of 3.69 THz and a temporal synthetic wavelength of 81.245 μm. As the laser frequency is sweeping, the integral interference phase variation is counted. Then, the fractional interference phases at the laser frequencies of 470.614 230 THz and 474.304 230 THz are measured respectively, by phase-shifting interferometry mentioned in section 3.1. Table 2 summarizes the measurement result of the integral diameter at 23.40 °C and 100.5 kPa. The integral diameter is 93.6238 mm by correcting to 20 °C and 101 kPa. Considering the frequency-sweeping range and the fractional phase measurement accuracy, the accuracy of the diameter is found to be 120 nm, which meets the requirement of the ambiguity range of phase-shifting interferometry.

Combing the average fractional measurement results in table 1 and the integral measurement result in table 2, the absolute diameter of the silicon sphere is found to be 93.623 712 at 20 °C and 101 kPa. In the Avogadro constant project, more than 70 diameters need to be measured to attain the mean diameter [4]. Note that only five diameters are measured in this experiment, because the long-term stability of the measurement environment is much worse. Nonetheless, the feasibility and repeatability of our interferometer have been demonstrated for a single diameter measurement.

3.3. Uncertainty evaluation

Table 3 shows the uncertainty budget for a single diameter measurement. First of all, the relative frequency uncertainty of the working laser is 9.2×10^{-12} in an averaging time of 0.03 s with tracing to an Rb clock, which is negligibly small in the uncertainty budget of the diameter measurement. An important contribution is from the interferogram analysis, including the uncertainty from the Carré phase-shifting algorithm and the standard deviation of the fractional phase measurement, which is related to the short-term stability of the measurement environment. Other negligible uncertainty sources are the beam alignment and the averaging region of selected pixels, which lead to a cosine error and a lateral error, respectively. By using the Gaussian beam tracing method [17, 18], the diffraction effect in our interferometer is estimated to be 0.02 rad. By measuring the mean thickness of the oxide layer using a spectroscopic ellipsometer calibrated by x-ray reflectivity, the mean thickness of the oxide layer is 4.23 nm with an uncertainty of 0.13 nm [30]. Surface roughness cannot be ignored in the diameter measurement. The uncertainty of the air refractive index during one diameter measurement process is estimated to be 2×10^{-8} by measuring the fluctuations of the temperature, atmospheric pressure, humidity and CO_2 composition. Apart from causing the uncertainty of the air refractive index, temperature fluctuation can also result in thermal expansion of the silicon sphere and the etalon, which is estimated to be 2.4 nm. Another major contribution comes from the diameter correction from the measurement statement to 20 °C and 101 kPa due to the uncertainty of the thermal expansion coefficient and compressibility coefficient of the silicon sphere. In short, the combined standard uncertainty is 5 nm and the diameter is found to be 93.623 712 mm at 20 °C and 101 kPa after the correction of the thickness of the oxide layer.

4. Conclusions

The phase-shifting interferometer based on a flat etalon and a traceable single laser frequency synthesizer is demonstrated in this paper to determine the absolute diameter of a silicon sphere for the Avogadro constant project. By using the OFC to calibrate the ECDL, the single laser frequency synthesizer can produce a tunable and stable laser frequency with a relative uncertainty of 9.2×10^{-12} in the range of 4 THz. Because the phase steps are generated by laser frequency tuning, the Carré algorithm with arbitrary but equal phase steps is used to calculate the fractional phases, whose uncertainty is a second-order small quantity. To overcome the ambiguity range of phase-shifting interferometry, the integral diameter is measured based on the principle of frequency-sweeping interferometry as the laser frequency is sweeping in a range of 3.69 THz, which corresponds to a temporal synthetic wavelength of 81.245 μm. Therefore, the absolute diameter is obtained by combining the integral and fractional diameter

measurement results. The absolute diameter is measured to be 93.623 712 mm with an uncertainty of 5 nm at 20 °C and 101 kPa. The uncertainty sources from the laser frequency and phase-shifting algorithm are reduced significantly. Because the diameter is measured in air, the main uncertainty sources come from the air refractive index and the thermal expansion of the silicon sphere. It can be foreseen that the target uncertainty demanded by the IAC project may be achieved by operating this interferometer in a vacuum chamber with rigorous temperature control.

Acknowledgments

This work was supported by Tsinghua University Initiative Scientific Research Program, the State Key Lab of Precision Measurement Technology and Instruments of Tsinghua University and the National Natural Science Foundation of China (grant no 51105227 and grant no 61205147).

References

[1] Becker P and Bettin H 2011 The Avogadro constant: determining the number of atoms in a single-crystal ^{28}Si sphere *Phil. Trans. R. Soc.* A **369** 3925–35
[2] Andreas B *et al* 2011 Counting the atoms in a ^{28}Si crystal for a new kilogram definition *Metrologia* **48** S1–13
[3] Johnson D P 1974 Geometrical considerations in the measurement of the volume of an approximate sphere *J. Res. Natl Bur. Stand.* A **78** 41–8
[4] Zhang J, Wu X and Li Y 2011 Uncertainty reevaluation in determining the volume of a silicon sphere by spherical harmonics in an Avogadro project *Chin. Phys.* B **20** 090601
[5] Kuramoto N, Fujii K, Nicolaus A, Bartl G, Gray M, Manson P and Giardini W 2011 Diameter comparison of a silicon sphere for the international Avogadro coordination project *IEEE Trans. Instrum. Meas.* **60** 2615–20
[6] Gläser M, Borys M, Ratschko D and Schwartz R 2010 Redefinition of the kilogram and the impact on its future dissemination *Metrologia* **47** 419–28
[7] Saunders J B 1972 Ball and cylinder interferometer *J. Res. Natl Bur. Stand.* C **76** 11–20
[8] Fujii K, Tanaka M, Nezu Y, Nakayama K, Masui R and Zosi G 1992 Interferometric measurements of the diameters of a single-crystal silicon sphere *Rev. Sci. Instrum.* **63** 5320–5
[9] Fujii K, Tanaka M, Nezu Y, Nakayama K and Masui R 1993 Accurate determination of the density of a crystal silicon sphere *IEEE Trans. Instrum. Meas.* **42** 395–400
[10] Luo Z, Gu Y, Zhang J, Yang L and Guo L 2010 Interferometric measurement of the diameter of a silicon sphere with a mechanical scanning method *IEEE Trans. Instrum. Meas.* **59** 2991–6
[11] Kuramoto N and Fujii K 2005 Volume determination of a silicon sphere using an improved interferometer with optical frequency tuning *IEEE Trans. Instrum. Meas.* **54** 868–71
[12] Nicolaus R A and Fujii K 2006 Primary calibration of the volume of silicon spheres *Meas. Sci. Technol.* **17** 2527–39
[13] Giardini W, Manson P, Wouters M, Warrington B, Ward B, Bignell N, Walsh C, Jaatinen E and Kenny M 2009 Density of a single-crystal natural silicon sphere *IEEE Trans. Instrum. Meas.* **58** 908–14
[14] Bartl G, Bettin H, Krystek M, Mai T, Nicolaus A and Peter A 2011 Volume determination of the Avogadro spheres of highly enriched ^{28}Si with a spherical Fizeau interferometer *Metrologia* **48** S96–103
[15] Kuramoto N, Fujii K and Yamazawa K 2011 Volume measurements of ^{28}Si spheres using an interferometer with a flat etalon to determine the Avogadro constant *Metrologia* **48** S83–95
[16] Malacara D, Serin M and Malacara Z 2005 *Interferogram Analysis for Optical Testing* (New York: Marcel Dekker)
[17] Andreas B, Ferroglio L, Fujii K, Kuramoto N and Mana G 2011 Phase corrections in the optical interferometer for Si sphere volume measurements at NMIJ *Metrologia* **48** S104–11
[18] Andreas B, Fujii K, Kuramoto N and Mana G 2012 The uncertainty of the phase-correction in sphere-diameter measurements *Metrologia* **49** 479–86
[19] Wu X, Zhang J, Wei H and Li Y 2012 Phase-shifting interferometer using a frequency-tunable diode laser calibrated by an optical frequency comb *Rev. Sci. Instrum.* **83** 073107
[20] Qian K, Shu F and Wu X 2000 Determination of the best phase step of the Carré algorithm in phase shifting interferometry *Meas. Sci. Technol.* **11** 1220–3
[21] Stoilov G and Dragostinov T 1997 Phase-stepping interferometry: five-frame algorithm with an arbitrary step *Opt. Lasers Eng.* **28** 61–69
[22] Novák J, Novák P and Mikš A 2008 Multi-step phase-shifting algorithms insensitive to linear phase shift errors *Opt. Commun.* **281** 5302–9
[23] Dorrío B V and Fernández J L 1999 Phase-evaluation methods in whole-field optical measurement techniques *Meas. Sci. Technol.* **10** R33–55
[24] Hibino K 1999 Error-compensating phase measuring algorithms in a Fizeau interferometer *Opt. Rev.* **6** 529–38
[25] Birch J E and Downs M J 1993 An updated Edlen equation for the refractive index of air *Metrologia* **30** 155–62
[26] Zhang J, Huang P, Li Y and Wei H 2013 Design and performance of an absolute gas refractometer based on a synthetic pseudo-wavelength method *Appl. Opt.* **52** 3671–9
[27] Lyon K G, Salinger G L, Swenson C A and White G K 1977 Linear thermal expansion coefficient of silicon from 6 to 340 K *J. Appl. Phys.* **48** 865–8
[28] Schödel R and Bönsch G 2001 Precise interferometric measurements at single crystal silicon yielding thermal expansion coefficients from 12 °C to 28 °C and compressibility *Proc. SPIE* **4401** 54–62
[29] Wu X, Wei H, Zhang H, Ren L, Li Y and Zhang J 2013 Absolute distance measurement using frequency-sweeping heterodyne interferometer calibrated by an optical frequency comb *Appl. Opt.* **52** 2042–8
[30] Zhang J, Li Y, Wu X, Luo Z and Wei H 2010 Determining mean thickness of the oxide layer by mapping the surface of a silicon sphere *Opt. Express* **18** 7331–9